Giant Number Fluctuations and Energy Spectra in 3-D Bacterial Turbulence

Zhengyang Liu, Wei Zeng, Xiaolei Ma, and Xiang Cheng
Department of Chemical Engineering and Materials Science,
University of Minnesota, Minneapolis, Minnesota 55455, USA
(Dated: November 21, 2020)

Giant number fluctuations, a landmark of collectively moving active particles, is universal in active systems across multiple length scales. Here, we present the first experimental study on the giant number fluctuation in 3-dimensional bacterial suspensions. Our measurements show that the number fluctuation scaled by the square root of mean number $\Delta N/\sqrt{N}$ scales with $N^{0.32}$ at high concentrations, confirming the theoretical predictions. Near the phase boundary, we observe a simultaneous increase of the scaling exponent and the flow induced by bacterial motions, suggesting a strong interplay between giant number fluctuations and flow. We show that this interplay spans all length scales in an active turbulence, by analyzing the kinetic energy spectra.

Giant number fluctuations (GNF), formally defined as the anomalously strong dependence of the variance of the number of particles on the mean number, is a universal phenomenon in active systems across multiple length scales, ranging from birds, fish and driven granules to bacteria, biological macromolecules and active synthetic particles [1–12]. Predicted by the seminal works from Toner and Tu [13–15], this phenomenon has stimulated extensive research interest and has become a landmark of ordered collectively moving particles [16–20].

Over the last 20 years, the understanding of GNF has been deepened significantly. Despite the progress, two important questions are still awaiting definite answers. First, the exact value of the scaling exponent of the variance on the mean has not reached an agreement. While the GNF is a seemingly universal in many systems, the scaling exponents measured or calculated in different systems show remarkable discrepancy [1, 6, 7, 9–12, 21–27]. In particular, the experimental works so far have reported scaling exponent ranging from 0.13 to 0.5 (the scaling exponent α is defined as $\Delta N/\sqrt{N} \propto N^{\alpha}$, ΔN is the standard deviation of particle number and N is the mean number) [1, 6, 7, 9–12], making it hard to compare experimental results with theory and simulations. We understand this situation by realizing that all the experiments have been done in 2-dimensional systems, with one or more frictional walls in direct contact to the active particles. We also notice that, although several experimental studies on bacterial systems have been reported, the GNF in bacterial turbulence - arguably the most fascinating and striking manifestation of microswimmer collective motions - has not been investigated (Supplementary movie 1 shows a vigorous bacterial turbulence in motion). Second, the driving force of GNF remains largely unclear. Although mechanisms based on nematic instability [1, 21, 22] and topological defects [9, 28] have been proposed or observed in specific systems, the driving force of GNF in other active systems, especially 3-dimensional systems dominated by hydrodynamic effects, remains unknown.

In this letter, we present an experimental measurement of GNF in 3-dimensional bacterial turbulence. Due to the absence of frictional walls, our results can provide a solid benchmark for other works to compare to. Meanwhile, our 3-D GNF measurement enables deeper studies on this universal phenomenon, such as the dimensionality effect. We also present a systematic measurement on the flow fields in active turbulence using particle image velocimetry (PIV), which has been shown to be a powerful tool in studying turbulent flows, and has been adopted to study active turbulence recently [9, 29–34]. Fig. 1d-e show the flow fields obtained from PIV analysis in dilute (1.6%) and dense (6.4%) bacterial suspensions. A detailed analysis on the velocity fields reveals a strong correlation between flow strength and GNF at multiple length scales.

Counting particle numbers poses a major challenge in measuring the GNF of 3-dimensional bacterial turbulence. Looking at the bright field microscopy images of a dense 3-dimensional bacterial suspension (Fig. 1c, and Supplementary movie 1), one immediately realizes that it is not possible to directly count the number of bacteria. Fortunately, the spatial distribution of bacterial concentrations can be inferred from optical microscopy images, where dark region indicates high local concentration and bright region indicates low local concentration. This idea is an extension of Beer-Lambert law which correlates solution concentration with its light attenuation. Similar principle has been used in some inspiring experimental works using image intensity as local concentration indicators [9, 35]. To be more quantitative on the relation between concentration and image pixel intensity, we did a calibration experiment by preparing bacterial suspensions of volume fractions ranging from 1.6% to 7.2% and take images of them under the same illumination. The images corresponding to different volume fractions are shown in Fig. 1a. As expected, when volume fraction gets higher, the image becomes dimmer. We plot the volume fractions as a function of the mean pixel intensities in the corresponding images, and find that the relation is almost linear, as shown in Fig. 1b.

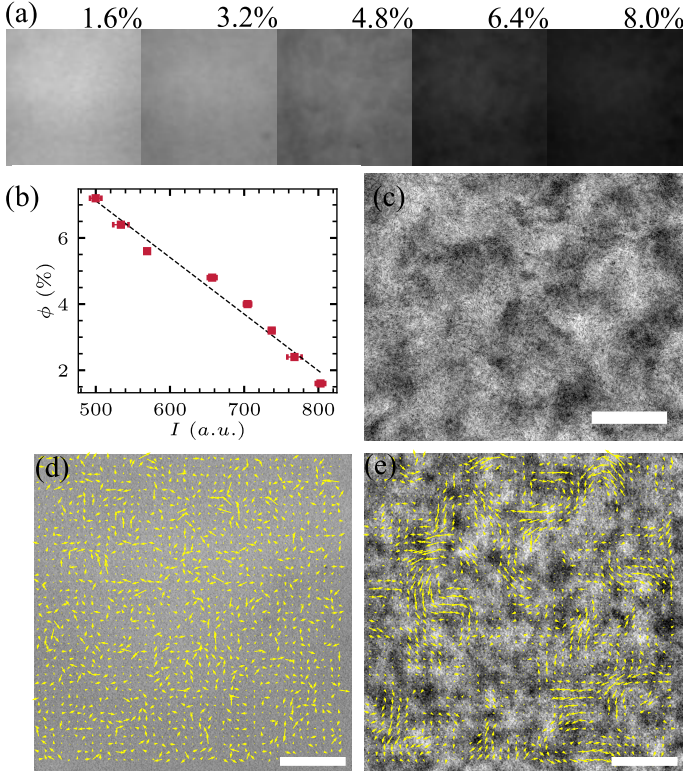With this linear relation, we are able to measure *rela-*

FIG. 1. (a) Bacterial suspensions of different volume fractions under the same illumination conditions. (b) Volume fraction as a function of averaged pixel intensities. (c) Bacterial active turbulence displaying constantly varying concentration inhomogeneity (6.4%). Scale bar is 100 µm. (d), (e) Velocity field of a dilute bacterial suspension (1.6%) and (6.4%). Scale bars are 135 µm.

tive local concentrations with image pixel intensities (see details in SM). We can in turn calculate the standard deviation of particle number ΔN and mean particle number N at in subsystems with various sizes. In Fig. 2a, we plot $\Delta N/\sqrt{N}$ as a function of l^2/l_b^2 for bacterial suspensions of volume fractions ϕ ranging from 0% to 9.6%. l is the side length of the square subsystems, and $l_b = 3$ µm is the length of a typical bacterial body. l^2/l_b^2 is thus a rescaled subsystem size and is proportional to mean particle number N. When $\phi < 3.2\%$, bacterial suspensions display a disordered state and standard deviation ΔN scales with $\sqrt{N}$, resulting in flat lines in Fig. 2a. When $\phi \geq 3.2\%$, bacterial suspensions start to exhibit a transition to turbulent state, and ΔN scales much faster than $\sqrt{N}$, exhibiting giant number fluctuations. If we write down the scaling relation between ΔN and N as $\Delta N \propto N^{0.5+\alpha}$, the excess exponent α quantifies the magnitude of GNF. For an equilibrium system, $\alpha = 0$; for a system displaying GNF, $\alpha > 0$ and α can take value up to 0.5. Note that beyond a *critical* length scale ($l^2/l_b^2 > 100$ or $l > 30$ µm), the all the curves in Fig. 2a level off due to the typical dynamics in bacterial active turbulence, which is

characterized by quasi-periodic formation and break-up of concentration patterns [25]. No GNF can be observed at such large length scales. When measuring α, we only look at the short length limit within 30 µm. By fitting for scaling exponents in Fig. 2a, we obtain α values at various volume fractions, as shown in blue markers in Fig. 2b. At low volume fraction limit, where no collective motion can be observed, α remains at a low level acround 0.05. As the volume fraction increases up to the turbulence transition ($\phi > 3.2\%$), α shows a gradual increase followed by a plateau above a volume fraction of 0.64. The α value at the high volume fraction limit is approximately 0.32.

In Fig. 2b, we also plot the kinetic energy of the flows E in bacterial suspensions at various volume fractions. E is calculated according to $E = \frac{1}{2}\langle|\boldsymbol{v}|^2\rangle$ from the velocity fields obtained by PIV. We find that α and E exhibit very similar concentration dependence. In particular, the increases of both α and E in the intermediate volume fractions $2.4\% < \phi < 6.4\%$ are almost concurrent, suggesting a strong correlation between these two quantities.
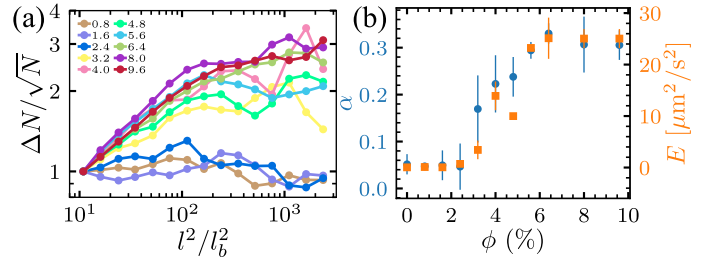

FIG. 2. **Concentration dependence of GNF.** (a) Standard deviation of particle number ΔN scaled by particle mean number N plotted against subsystem size rescaled by single bacterium size l^2/l_b^2 in bacterial suspensions at volume fractions ranging from 0.8% to 9.6%. (b) Concentration dependence of the magnitude of GNF α (blue circles) and kinetic energy E (orange squares).

The correlation between α and E mentioned above is found on the length scale of the whole field of view. To further investigate the correlation between GNF and flow kinetic energy, we examine the *local* correlation between concentration fluctuations and kinetic energy at a much smaller length scale. To do it, we divide the images of bacterial suspensions taken with bright field microscope into small windows using the same dividing scheme as the PIV interrogation window, as shown in Fig. 3a.

[1] V. Narayan, S. Ramaswamy, and N. Menon, Science **317**, 105 (2007), arXiv:0612020 [cond-mat].

[2] I. Aranson, A. Snezhko, J. S. Olafsen, and J. S. Urbach3, **320**, 1 (2008).

[3] A. J. Ward, D. J. Sumpter, I. D. Couzin, P. J. Hart, and

J. Krause, Proceedings of the National Academy of Sciences of the United States of America **105**, 6948 (2008).

[4] M. Ballerini, N. Cabibbo, R. Candelier, A. Cavagna, E. Cisbani, I. Giardina, V. Lecomte, A. Orlandi, G. Parisi, A. Procaccini, M. Viale, and V. Zdravkovic, Proceedings of the National Academy of Sciences of the United States of America **105**, 1232 (2008).

[5] A. Sokolov, R. E. Goldstein, F. I. Feldchtein, and I. S. Aranson, Physical Review E - Statistical, Nonlinear, and Soft Matter Physics **80**, 1 (2009).

[6] J. Deseigne, O. Dauchot, and H. Chaté, Physical Review Letters **105**, 1 (2010), arXiv:1004.1499.

[7] H. P. Zhang, A. Be'er, E. L. Florin, and H. L. Swinney, Proceedings of the National Academy of Sciences of the United States of America **107**, 13626 (2010).

[8] J. Palacci, S. Sacanna, A. P. Steinberg, D. J. Pine, and P. M. Chaikin, Science **339**, 936 (2013).

[9] V. Schaller and A. R. Bausch, Proceedings of the National Academy of Sciences of the United States of America **110**, 4488 (2013).

[10] D. Nishiguchi, K. H. Nagai, H. Chaté, and M. Sano, Physical Review E **95**, 1 (2017), arXiv:1604.04247.

[11] K. Kawaguchi, R. Kageyama, and M. Sano, Nature **545**, 327 (2017).

[12] H. Karani, G. E. Pradillo, and P. M. Vlahovska, Physical Review Letters **123**, 208002 (2019).

[13] J. Toner and Y. Tu, Physical Review Letters **75**, 4326 (1995), arXiv:9506001 [adap-org].

[14] Y. Tu, J. Toner, and M. Ulm, Physical Review Letters **80**, 4819 (1998).

[15] J. Toner and Y. Tu, Physical Review E - Statistical Physics, Plasmas, Fluids, and Related Interdisciplinary Topics **58**, 4828 (1998), arXiv:9804180 [cond-mat].

[16] J. Toner, Y. Tu, and S. Ramaswamy, Annals of Physics **318**, 170 (2005).

[17] S. Ramaswamy, Annual Review of Condensed Matter Physics **1**, 323 (2010), arXiv:1004.1933.

[18] T. Vicsek and A. Zafeiris, Physics Reports **517**, 71 (2012), arXiv:1010.5017.

[19] D. Saintillan and M. J. Shelley, Comptes Rendus Physique **14**, 497 (2013).

[20] M. C. Marchetti, J. F. Joanny, S. Ramaswamy, T. B. Liverpool, J. Prost, M. Rao, and R. A. Simha, Reviews of Modern Physics **85**, 1143 (2013), arXiv:1207.2929.

[21] R. Aditi Simha and S. Ramaswamy, Physical review letters **89**, 058101 (2002), arXiv:0108301 [cond-mat].

[22] S. Ramaswamy, R. A. Simha, and J. Toner, Europhysics Letters **62**, 196 (2003), arXiv:0208573 [cond-mat].

[23] H. Chaté, F. Ginelli, G. Grégoire, and F. Raynaud, Physical Review E - Statistical, Nonlinear, and Soft Matter Physics **77**, 1 (2008), arXiv:0712.2062.

[24] S. Dey, D. Das, and R. Rajesh, Physical Review Letters **108**, 1 (2012).

[25] D. Saintillan and M. J. Shelley, Journal of the Royal Society Interface **9**, 571 (2012).

[26] S. Ngo, A. Peshkov, I. S. Aranson, E. Bertin, F. Ginelli, and H. Chaté, Physical Review Letters **113**, 1 (2014), arXiv:1312.1076.

[27] B. Mahault, F. Ginelli, and H. Chaté, Physical Review Letters **123**, 1 (2019), arXiv:1908.03794.

[28] D. Saintillan and M. J. Shelley, Physics of Fluids **20**, 10.1063/1.3041776 (2008).

[29] T. Ishikawa, N. Yoshida, H. Ueno, M. Wiedeman, Y. Imai, and T. Yamaguchi, Physical Review Letters **107**, 1 (2011).

[30] H. H. Wensink, J. Dunkel, S. Heidenreich, K. Drescher, R. E. Goldstein, H. Löwen, and J. M. Yeomans, Proceedings of the National Academy of Sciences of the United States of America **109**, 14308 (2012), arXiv:1208.4239v1.

[31] A. Sokolov and I. S. Aranson, Physical Review Letters **109**, 1 (2012), arXiv:0710.3256v2.

[32] T. Sanchez, D. T. Chen, S. J. Decamp, M. Heymann, and Z. Dogic, Nature **491**, 431 (2012).

[33] J. Dunkel, S. Heidenreich, K. Drescher, H. H. Wensink, M. Bär, and R. E. Goldstein, Physical Review Letters **110**, 1 (2013), arXiv:1302.5277.

[34] Y. Peng, Z. Liu, and X. Cheng, Imaging the emergence of bacterial turbulence using light-powered Escherichia coli (2020).

[35] L. G. Wilson, V. A. Martinez, J. Schwarz-Linek, J. Tailleur, G. Bryant, P. N. Pusey, and W. C. Poon, Physical Review Letters **106**, 7 (2011), arXiv:1004.4764.
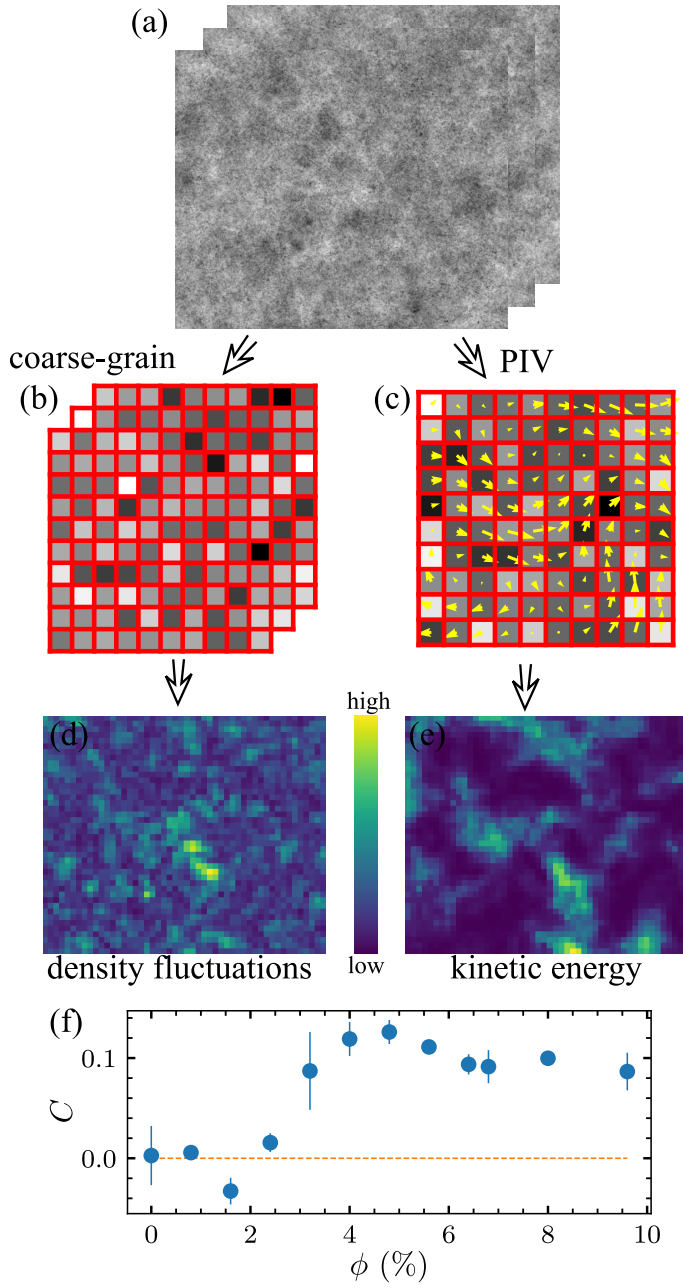
FIG. 3. **Calculation of local correlation between density fluctuations and kinetic energy.** (a) An image stack of bacterial active turbulence ($\phi = 4.8\%$). (b) Divide images into small windows and average the pixel intensities to "coarse-grain" the image (c) PIV analysis on the same dividing scheme as in (b). (d) Local density fluctuations, defined as standard deviations of averaged pixel intensities in each window. (e) Local kinetic energy, defined as half of squared velocity in each window . (f) Cross correlation between local density fluctuations and local kinetic energy C plotted against volume fraction ϕ.